The First High Solar Concentrator System Performance Test in Korea

Kyung-Yul Chung[†] · Sung-Won Kang[1] · Yong-Sik Kim[2] · Chang-Ho Sim[3] ·
Nam-Young Jeong[4] · Chang-Dae Park[5] · Keel-Soo Ryu[6]

Abstract：The worldwide CPV(Concentrated Photo Voltaic) market has been increased rapidly due to the increase in large-scale PV(Photo Voltaic) plants which are situated in sun-rich areas with either a Mediterranean or equatorial-type climate. CPV systems are arguably some of the most important devices in the production of electricity within regions with a sun-rich climate, particularly those which benefit from abundant direct solar irradiation. We have developed a 500X CPV module with rated power of 170Wp. The CPV module must satisfy the constraint of having a sensitive tracking accuracy due to the limited tolerance of the acceptance angle in intrinsic optical design. In this study, the module's acceptance angle used was designed with a tolerance angle of ±1° in the secondary optics design. In general, non-concentrated module type 2-axis trackers have a tolerance angle larger than ±1° due to standard silicon-type modules which are insensitive to the tracking accuracy of the sun. They have a tolerance angle of ±2~4°, which fails to exert a significant influence on the performance of the module. This paper provides a study of an experimental variation of the efficiency of the CPV module in terms of its tracking accuracy. Also, the performance of the module is studied from the perspective of temperature and direct irradiation.

Key words：*CPV* module test, tolerance angle, 2-axis trackers

1. Introduction

Today, though the photovoltaic industry is growing rapidly, it is still faced by the limitations of requiring high-cost photovoltaic systems, particularly the expensive solar cell. An effective way to reduce system cost is to reduce the amount of solar cells by means of combining them with concentrating optics such as Fresnel lenses or mirrors. CPV systems might be more profitable solutions than general silicon-type PV systems in sun-rich regions such as in California or areas of

----

[†] Corresponding Author(Kyung-Yul Chung, Korea Institute of Machinery and Materials, 156 Gajungbukno, Yuseonggu, Daejeon, 305-343, Korea, E-mail: kychung@kimm.re.kr, Tel: 82-42-868-7333)

1 Sungwon Kang, R&BD Center, BJ Power Co., Ltd, Daejeon, Korea, Tel: 82-42-273-7460, E-mail: swkang@bjpower.co.kr,

2 Yongsik Kim, Business Center, BJ Power Co., Ltd, Daejeon, Korea, E-mail: yosikim@bjpower.co.kr, Tel: 82-42-273-7460

3 Changho Sim, Production Center, BJ Power Co., Ltd, Daejeon, Korea, E-mail: chsim@bjpower.co.kr, Tel: 82-42-273-7460

4 Nam Young Jeong, Graduate School of Energy and Environment, Seoul National University of Science and Technology, Seoul, Korea, E-mail: powerjny@naver.com, Tel: 82-41-680-7627

5 Chagdae Park, Energy Plant Research Division, Korea Institute of Machinery and Materials, 156 Gajungbukno, Yuseonggu, Daejeon, 305-343, Korea, E-mail: parkcdae@kimm.re.kr, Tel: 82-42-868-7333

6 Keel-Soo Ryu, Division of Information Technology, Korea Maritime Univ., 727 Taejong-ro, Yeongdo-Gu, Busan, 606-791, Korea, E-mail: rhyu@hhu.ac.kr, Tel: 82-51-410-4571

the Middle East. CPV systems are a better candidate for early grid parity achievement than other renewable energy systems in sun-rich regions with direct irradiations. In order to expand various domestic PV markets and confirm the possibility of CPV module performance within Korea, a performance test was carried out on the CPV Module. This study used a 170Wp module with a 500X concentration Fresnel lens and tested module performance with a 2-axis tracker. The relationship between the efficiency and temperature of the module was tested through an electricity performance test and a temperature test. Additionally, the relationship between tracking error and module efficiency was also checked. Through these procedures, the influence of tracking error of 2-axis tracker on the module performance was able to be investigated. An improvement in module efficiency can be realized by increasing the secondary optics tolerance angle and the exact tracking correction of the 2-axis tracker.

2. Background of Fresnel lens optics
2.1 Lens formula

The PV concentration system is largely divided into two categories: mirror type concentration systems and lens type concentration systems. In this paper, we deal with ray tracing simulation with a primary Fresnel lens and secondary truncated light pipe.

Imaging Fresnel lens design follows the same principles of geometrical optics that are also used in the design of other lenses, particularly the concepts of focal length and aperture. The design of some simple Fresnel lenses will be presented to enable the evaluation of focusing lenses for use as solar collectors. The f/# is a measure of the aperture of the lens. The f is the focal length and # represents number. It describes the ratio of the effective focal length to the diameter of the lens. The f/# is a measure of the flux concentration of the imaging lens. As the geometrical concentration ratio $C \rightarrow \infty$, the energy flux in the focal point is related to the amount of radiation concentrated.

$$f/\# = f/2R \tag{1}$$

where R denotes the distance of the extreme paraxial ray from the optical axis of the system.

A typical imaging Fresnel lens with grooves facing inwards is presented here. Refractive index is n. The prism angle α is the goal of a simulation, as shown in [1]

$$
\begin{aligned}
n\sin\alpha &= \sin\beta \\
\tan\omega &= \frac{R}{f} \\
\beta &= \alpha + \omega
\end{aligned}
\tag{2}
$$

From (2), we can give a final expression for the prism angle α in terms of focal length f and aperture R:

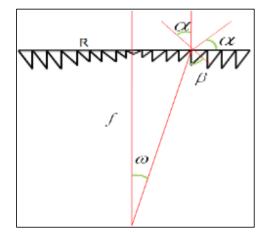$$\tan\alpha = \frac{R}{n\sqrt{R^2 + f^2} - f} \tag{3}$$

Figure 1: general Fresnel lens with grooves facing inward

The fraction of the incident power that is reflected from the interface is given by the reflectance R and the fraction that is refracted is given by the transmittance T. The media are assumed to be *non-magnetic*.

The calculations of R and T depend on polarization of the incident ray. If the light is polarized with the electric field of the light perpendicular to the plane of (*s*-polarized), the reflection coefficient is given by [2].

$$R_s = \left(\frac{n_f \cos \theta_i - n_{air} \cos \theta_t}{n_f \cos \theta_i + n_{air} \cos \theta_t} \right)^2$$

$$= \left[\frac{n_f \cos \theta_i - n_{air} \sqrt{1 - \left(\frac{n_f}{n_{air}} \sin \theta_i \right)^2}}{n_f \cos \theta_i + n_{air} \sqrt{1 - \left(\frac{n_f}{n_{air}} \sin \theta_i \right)^2}} \right]^2 \quad (4)$$

If the incident light is polarized in the plane of (*p*-polarized), the R is given by [2]

$$R_p = \left(\frac{n_f \cos \theta_t - n_{air} \cos \theta_i}{n_f \cos \theta_t + n_{air} \cos \theta_i} \right)^2$$

$$= \left[\frac{n_{air} \sqrt{1 - \left(\frac{n_f}{n_{air}} \sin \theta_i \right)^2} - n_f \cos \theta_i}{n_{air} \sqrt{1 - \left(\frac{n_f}{n_{air}} \sin \theta_i \right)^2} + n_f \cos \theta_i} \right]^2 \quad (5)$$

$$T_{top} = \frac{4 n_{fr}}{(1 + n_{fr})^2}$$

$$T_s = 1 - R_s$$
$$T_p = 1 - R_p$$

$$T_{total} = T_{top} * \frac{T_s + T_p}{2} \quad (6)$$

Total optical efficiency can be calculated from [6].

2.2 Lens test and simulation result

A sample Fresnel lens was developed with a focal length of 280mm. The sample Fresnel lens performance was tested in order to certify the optical efficiency of the lens.

Figure 2: Fresnel lens performance test

In outdoor testing, a higher performance was gained through using focal depths greater than 280mm. This could be due to the lens forming a tight focal spot in the centre of the cell and causing hot spotting. In this case, an increase in the focus distance leads to a more even light distribution across the cell and a resultant higher power output. This means that the optimal distance between the lens and the cell could be longer. Nonetheless, the focal depth used in the design remains 280mm.

The focal depth is the distance to the optimum focal spot. The optimum distance to place the lens from the cell can differ from this depending on the setup and configuration of the system.

Previous analysis undertaken by the authors suggested that the optimal distance from the cell to the lens is in the region of 255mm. That is shorter than the design focal length. This could be explained by the nature of the light source used differing from that of the 'actual sun'. Most solar simulation sources cannot match the sun in terms

of the spectrum average of degree of collimation, which thus tends to result in a different optimal distance from the lens to the cell. If a non-solar simulation source is used, the focal length will vary from that of the design length depending on how different the light source is.

In other research institution test setups [3], an LED light source is used which in no way matches the solar spectrum. In such setups, the distance from the lens to the cell is sought to be optimized through a process of trial and error; the actual distance is thus ignored as irrelevant. Such testing is designed to understand the quality of the Fresnel lens structure, rather than its performance in real solar conditions.

By contrast, the assumptions used in this study were that the secondary would have an acceptance area of between 15mm by 15mm and 20mm by 20mm. Accordingly, a lens was designed with the given focal length and a measurement was made of the level of light incident to this area at a 280mm focal length. These were the numbers provided in this study. This does not mean that the optimum distance between the lens and the cell would remain 280mm if the lens were to be used with a 1cm cell without a secondary.

2.3 Modelled performance at different focal lengths

The analysis below shows the effect of placing the lens at different distances from the cell. As can be seen, the total efficiency over the 15mm by 15mm cell area is optimised at 280mm as expected. Nonetheless, a closer analysis of the spot spread reveals a more complex picture.

At a distance of 255mm, the focal spot is extremely large (over 25 mm), meaning that the efficiency is low.

At a distance of 270mm, the focal spot is about 12mm wide, as can be seen. Though not shown in

the diagram, there is still some light lost, which means that efficiency is not optimised. However, as the light is spread more evenly across the cell, this configuration may produce a higher power output in a field test, given that there is less hot spotting.
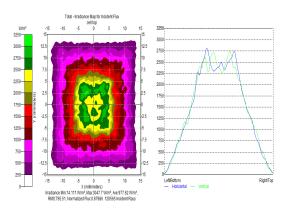
Efficiency is maximized at a distance of 280mm as the most light possible hits the cell. Notwithstanding this, in real life the power output may be reduced due to the occurrence of hot spotting.

These figures all relate to a focal spot sized at 15mm by 15mm. Analysis was also redone with a 10mm by 10mm spot size, showing that efficiency loss increases more rapidly, the more the optimum focal depth is moved.
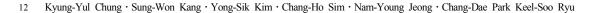
A second significant point to note is that it is not possible to replicate these results with an in-door set up as it is not possible to accurately simulate actual solar conditions.
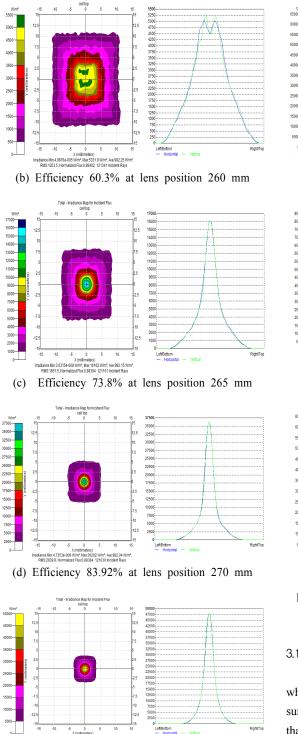
2.4 Distributions at different positions

In this simulation, solar spectral weight was applied. In order to give an overall idea of distribution, the pictures are distributed on an area of 30 mm by 30 mm, but the efficiencies are still measured on a 15 mm by 15mm area.
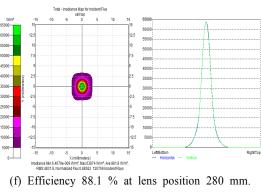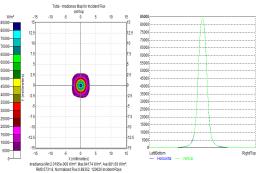

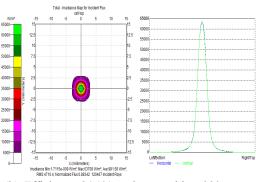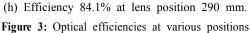(a) Efficiency 48.12% at lens position 255 mm

(b) Efficiency 60.3% at lens position 260 mm

(f) Efficiency 88.1 % at lens position 280 mm.

(c) Efficiency 73.8% at lens position 265 mm

(g) Efficiency 87.6% at lens position285 mm.

(d) Efficiency 83.92% at lens position 270 mm

(h) Efficiency 84.1% at lens position 290 mm.

Figure 3: Optical efficiencies at various positions

3. CPV Module performance test

3.1 Temperature performance test of CPV module

A sun tracking operation was used to test whether a 2-axis tracker tracks the position of the sun precisely or not. The observations taken show that the 2-axis tracker tracks off ± 1˚of the exact position of the normal to the sun.

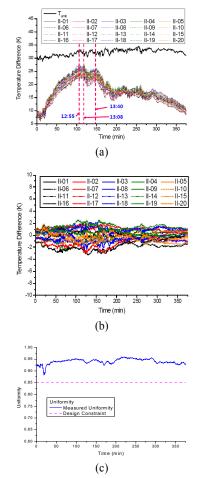(e) Efficiency 87.8% at lens position 275 mm

(a)

(b)

(c)

Figure 4: Thermal performance of module with time in the outdoor test

Data was collected from a program developed in-house to monitor module performance. The module attached temperature sensors collect data using Agilent DAQ. The total cooling system through a thermal performance evaluation of the CPV module showed an average atmospheric temperature range of 30℃ ~ 35℃ and a maximum temperature difference of 28℃. The cooling design used for the CPV module was fixed to a ΔT<40 ℃ between the rear side temperature of the cell and the atmospheric temperature. Additionally, temperature uniformity was over 85%.

Figure 4 (a) shows 20 graphs of cell temperature

difference and daily average temperatures. It shows a maximum temperature deviation of 3.3 ℃ from the average temperature. **Figure 4** (b) shows the result of average cell temperatures and temperature differences. **Figure 4** (c) represents the result of temperature uniformity over time. As shown in **Figure 4** (a), the maximum temperature difference between cells and the atmosphere was 28℃, which was lower than that of the simulation result of the thermal analysis. The simulation result of the maximum temperature difference was 34.97℃. This thus indicates that heat energy generation per unit cell is less than 17W. The calculation of heat energy of unit cell is shown in **Table 1**.

Table 1: Estimated calculation of heat generation of solar cell [*average reflectance of single SiN AR coating and DL(Dual layer)SiN AR coating [4]]

CASE	DNI×Lens optical efficiency×lens area ×(1-reflectivity*)×(1-cellefficiency)	Heat energy generation
Primary Lens Only (Lens optical efficiency: 80%)	800W/m²×0.8×0.224²m²×(1-0.127) ×(1-0.35)	18W
	850W/m²×0.8×0.224²m²×(1-0.127) ×(1-0.35)	19W
	900W/m²×0.8×0.224²m²×(1-0.127) ×(1-0.35)	21W
Primary Lens/Secondary Lens (Optical efficiency: 80%/85%)	800W/m²×0.68×0.224²m²×(1-0.127)×(1-0.35)	15W
	850W/m²×0.68×0.224²m²×(1-0.127)×(1-0.35)	16W
	900W/m²×0.68×0.224²m²×(1-0.127)×(1-0.35)	**17W**

3.2 Performance test result and its power loss factor analysis

The CPV module used in this study had 20 receivers attached to the chemical compound triple junction solar cells with primary optics (500X Fresnel lens) and secondary optics. In addition, it had 20 heat sinks in the rear side of the center of each cell region. It was given a rated maximum power of 170Wp.
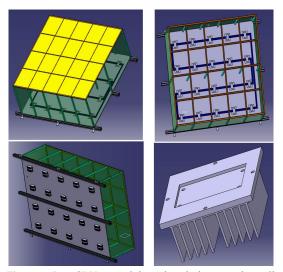
Figure 5: CPV module description and cell arrangement

Figure 5 represents 4 by 5 cell arrangements in the CPV module. The total area is 0.9m by 1.124m. From one cell unit test, the maximum power peak was 8.5Wp. This study initially estimated the power of the 20 cell unit at 170Wp. According to this estimation, a CPV module was set up with a rate power of 170Wp.
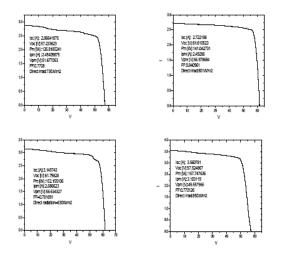

Figure 6: Measured CPV module powers with direct irradiations.

Figure 6 represents measured CPV module power

with direct irradiation. Its power increases with the rise of direct irradiation. The measured power profile from the I-V curve is less than the designed one. The rise in the temperature of the module results in reductions to cell efficiency and a consequent decrease in its power output.

Secondary optics were designed in consideration of the tracking error of ±1°due to the incorrect tracking of the sun position on the 2-axis tracker. The design of the CPV module has a maximum power peak at the normal to the sun. The simulation result of this study shows that tracking errors result in a great loss of optical efficiency when secondary optics are not used.
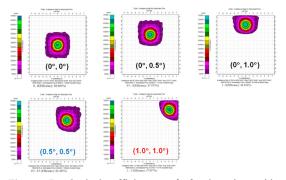

Figure 7: Optical efficiency of focal point with tolerance angle in the Fresnel lens

Figure 7 represents optical efficiency of Fresnel lens with tracking errors.

Figure 8 shows that secondary optics can compensate for a reduction in CPV module performance due to a reduction of optical loss of tracking error. Figure 6 show that the average cell intensity with a tracking error of 1° is 92% of the normal average.

Figure 8 (a) and **(b)** show light distribution on a cell size of 10mm^2 in the case of a tracking error of 1° and no tracking error, respectively.

Simulation data shows that average cell intensity without a tracking error is 76.02W/mm^2 in

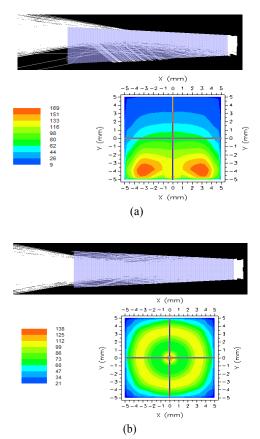comparison with an average of $70.7W/mm^2$ in the case of tracking error of 1°.

(a)

(b)

Figure 8 : Secondary optics simulation result of tolerance angle of 1°
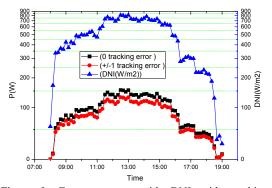

Figure 9: Energy output with DNI with tracking error of 0° and 1°

Figure 9 represents the measured output energy

data of the CPV module. A CPV 2-axis tracker produced in TAIWAN was used. The tracking error was calculated using a DNI Pyrheliometer by measuring how much sun light tracks off the pinhole central point.

The blue line indicates that DNI(Direct Normal Irradiation) varies according to the time of day. The black line indicates that CPV module power varies with DNI(Direct Normal Irradiation) in the case of having no tracking error. By contrast, the red line shows that CPV module power varies with DNI(Direct Normal Irradiation) in the case of a tracking error of ±1°. Our measured result of energy output in **Figure 9** correlates well with the simulation one shown in **Figure 8**.

4. Conclusions

The results of this study are that 2-axis trackers must have an accurate tracking condition with minimal tracking errors. Moreover, in order to reduce the loss of CPV module performance, secondary optics must have a larger tolerance angle and a 2-axis tracker must have improved accuracy. Various kinds of additional experiments are required to verify the quantitative analysis of low short currents caused by optical losses, current mismatches of multi-junction solar cells from measured solar spectrums and calibration errors caused by tracker arrangements [5]. This paper, as stated above, has focused on the major factor of energy output loss, as analyzed as an optical efficiency loss caused by a tracking error. The tracking error raises the problem of non-uniform illumination and temperature distribution in each cell, which may lead to the growth of series resistance in each cell and a consequent energy output reduction. Moreover, it is likely to cause the insulation breakdown of each cell due to a long-term temperature rise of non-uniform cell illumination. Current mismatching and non-uniform

temperature distribution causes a total energy loss in the CPV module. First and foremost, this paper has evaluated how to make a correction to the tracking error problem extant in the 2-axis tracker. The following papers shall turn to the issues raised in the experiments mentioned above and suggest ways of solving the tracking problems caused.

References

[1] R. Leutz and A. Suzuki, Nonimaging Fresnel Lenses: Design and Performance of Solar Concentrators, Springer, 2001.

[2] Max Born and Emil Wolf, Principles of Optics, 7th Edition, Cambridge University Press, Cambridge, United Kingdom, 2002.

[3] Kwang-sun Ryu et al., "Optical design and manufacturing of Fresnel lenses for the first korean high concentration solar PV system", Proceedings of the International Conference on Concentrating Photovoltaic systems (CPV-7), pp. 101-104, April 2011.

[4] B. Kumar, T. B. Pandian, E. Sreekiran, and S. Narayanan, "Benefit of dual layer silicon nitride antireflection coating," in Proceedings of the IEEE Conference on Photovoltaic Specialists, pp. 1205-1208, 2005.

[5] S. Kurtz, "Opportunities and challenges for development of a mature concentrating photo voltaic power industry", Technical report of NREL(National Renewable Energy Laboratory) / TP-520-43208, 2009.